THE JOURNAL OF PHYSICAL CHEMISTRY B

pubs.acs.org/JPCB Article

Dynamic Nuclear Polarization with Electron Decoupling in Intact Human Cells and Cell Lysates

Patrick T. Judge, Erika L. Sesti, Lauren E. Price, Brice J. Albert, Nicholas Alaniva, Edward P. Saliba, Thomas Halbritter, Snorri Th. Sigurdsson, George B. Kyei, and Alexander B. Barnes*

Cite This: J. Phys. Chem. B 2020, 124, 2323–2330 Read Online

ACCESS | Metrics & More | Article Recommendations | Supporting Information

ABSTRACT: Dynamic nuclear polarization (DNP) is used to improve the inherently poor sensitivity of nuclear magnetic resonance spectroscopy by transferring spin polarization from electrons to nuclei. However, DNP radicals within the sample can have detrimental effects on nuclear spins close to the polarizing agent. Chirped microwave pulses and electron decoupling (eDEC) attenuate these effects in model systems, but this approach is yet to be applied to intact cells or cellular lysates. Herein, we demonstrate for the first time exceptionally fast ^{1}H T_{1DNP} times of just 200 and 300 ms at 90 and 6 K, respectively, using a newly synthesized methylated trityl radical within intact human cells. We further demonstrate that eDEC can also be applied to intact human cells and human and bacterial cell lysates. We investigate eDEC efficiency at different temperatures, with different solvents, and with two trityl radical derivatives. At 90 K, eDEC yields a ^{13}C signal intensity increase of 8% in intact human cells and 10% in human and bacterial cell lysates. At 6 K, eDEC provides larger intensity increases of 15 and 39% in intact human cells and cell lysates, respectively. Combining the manipulation of electron spins with frequency-chirped pulses and sample temperatures approaching absolute zero is a promising avenue for executing rapid, high-sensitivity magic-angle spinning DNP in complex cellular environments.

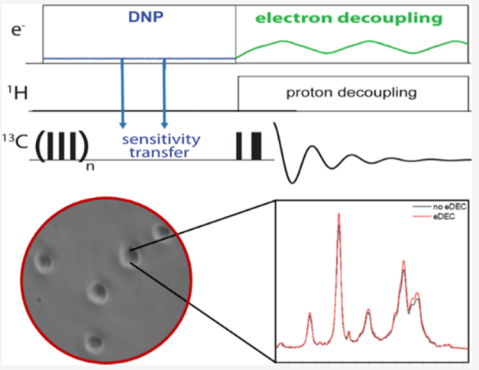

INTRODUCTION

Solid-state nuclear magnetic resonance (NMR) is a valuable method for studying biological systems at atomic resolution;[1−7] however, it suffers from an inherent lack of sensitivity.[8−10] In complex biological environments, NMR sensitivity is further challenged by low endogenous cellular concentrations of molecules of interest. Dynamic nuclear polarization (DNP) can increase NMR sensitivity by orders of magnitude by transferring spin polarization from electron paramagnetic resonance (EPR)-active polarizing agents to target nuclear spins.[11−20] While polarizing agents for DNP boost polarization, they can also cause deleterious paramagnetic effects such as shorter coherence lifetimes (line broadening) and signal attenuation.[21−24] These effects become more severe as hyperfine interactions increase. Recently, we introduced a strategy to attenuate hyperfine couplings by decoupling electron−nuclear interactions with frequency-chirped microwave pulses generated by a frequency-agile gyrotron.[25,26] Electron decoupling (eDEC) has been successfully applied to model systems of small molecules suspended in a cryoprotecting glassy matrix (glycerol-d_8/D_2O/H_2O, 60/30/10%).[25,27] Extending eDEC to more complex samples is important for translational studies in biological systems.

Establishing the structure−function relationship of molecular architectures of interest is fundamental to many biological studies. Reductive approaches are often employed to study biomolecular structures in simplified environments in vitro. However, proteins, drugs, and biomolecules of biomedical importance do not necessarily have the same behavior, or structural ensembles, in simple in vitro environments as they do in the cellular context or in vivo environments. Recent studies have demonstrated the profound effect of the complex cellular environment on the protein structure.[28,29]

Complex mixtures also have significant effects on DNP efficiency.[30] While different formulations can be detrimental to DNP in vitro, we recently demonstrated an excellent DNP performance in intact human cells.[31] To transition eDEC with DNP to in-cell structural biology, the efficacy of eDEC must be demonstrated in more complex cellular environments. Chirped microwave pulses, which improve control over electronic and hyperfine interactions within the Hamiltonian, are a promising route to improve in-cell NMR. Here, we perform effective eDEC in isotopically enriched intact human cells and human

Received: November 8, 2019
Revised: February 10, 2020
Published: February 21, 2020

https://dx.doi.org/10.1021/acs.jpcb.9b10494
J. Phys. Chem. B 2020, 124, 2323−2330

and bacterial cell lysates at 90 and 6 K with two different trityl radicals (Finland trityl radical and trityl-Me_3N). Trityl-Me_3N is a newly synthesized polarizing agent designed to shorten magnetization recovery delays.[32,33] We present exceptionally short ^1H T_{1DNP} times with the trityl-Me_3N radical in intact human cells below 6 K.

EXPERIMENTAL METHODS

Solid Effect Radicals. Two tertiary carbon stable organic radical-containing compounds, Finland trityl radical (Oxford Instruments, Concord, MA) and trityl-Me_3N were investigated. Trityl-Me_3N was synthesized as described in the Supporting Information Section S3. While eDEC has been successfully applied to model systems, it has yet to be demonstrated within intact cells. Direct DNP transfers and eDEC within intact cells require penetration of DNP polarizing agents through the membranes and distribution throughout the cells. In addition to the Finland trityl radical, we also explored the use of trityl-Me_3N. The trityl-Me_3N derivative was synthesized and deployed in this study to exploit the additional advantages of the methyl groups, leading to faster replenishing of magnetization (shorter ^1H T_{1DNP}) and higher sensitivity experiments.[34]

Human Cell Lysate Preparation. For human cell lysates, Jurkat T cells (ATCC, Manassas, VA) were cultured in a [U-^{13}C, 98%; U-^{15}N, 98%] BioExpress-6000 mammalian cell-growth medium (Cambridge Isotope Laboratories, Tewksbury, MA) at a concentration of 3×10^6 cells/mL in a six-well plate at 37 °C and 5% CO_2 for 48 h. 4.0×10^7 cells were collected, spun at 170g for 5 min, washed with 1× phosphate-buffered saline (PBS), and spun again at 170g for 5 min to remove extracellular NMR labels. A solution was prepared for DNP cryoprotection and cell lysis by dissolving 40 mM Finland trityl radical in a solution of 60% glycerol-d_8, 30% D_2O, and 10% H_2O (cryoprotecting glassy matrix). Triton X-100 was added to the final concentration of 0.5 v/v % to lyse the cells. A cryoprotecting matrix (30 μL) combined with cell lysis solution was added to the cell pellet, and 36 μL of the resulting suspension was added to a 3.2 mm zirconia rotor and frozen in liquid nitrogen.

Intact Human Cell Preparation. Jurkat cells for intact human cell experiments were cultured and washed under the same conditions as the Jurkat cells for the lysed samples, except cells were plated at 2×10^6 cells/mL and 3.6×10^7 cells were collected for each experiment. The cell pellet was resuspended in 36 μL of 1× PBS with 10% dimethyl sulfoxide containing either 40 mM Finland trityl radical or trityl-Me_3N radical. This suspension was centrifuged directly into the 3.2 mm zirconia rotor at 800g for 30 s and immediately frozen in liquid nitrogen as detailed in our previous work.[31]

Bacterial Cell Lysate Preparation. Rosetta electrocompetent *Escherichia coli* (*E. coli*) cells electroporated with a PGEX-4T plasmid (GenScript, Piscataway, NJ) bearing an insert coding for the C1b domain of the δ isoform of protein kinase C (PKC-δ) were incubated in the super optimal broth (S.O.C.) medium for 1 h before plating on a selective medium. The colonies obtained were then cultured in 200 mL of a ^{15}N-, ^{13}C-, and ^2H-labeled ISOGROW complex medium (Sigma-Aldrich, St. Louis, MO) until the 600 nm optical density reached the midlog point (0.6). Then, the culture was induced and left to incubate and grow overnight at 20 °C. The cells were collected by centrifugation. All buffers were completely deuterated to minimize the ^1H concentration. The pellets were lysed in lysis buffer by sonication, and the lysate was then centrifuged. The soluble fraction was decanted, steri-filtered, and incubated for 2.5 h at room temperature with 1.2 mL of glutathione-*S*-transferase (GST) beads (Thermo Fisher Scientific, Waltham, MA) to isolate the GST-PKC C1b from the soluble fraction. The beads were then centrifuged at 600g for 4 min, and the supernatant was removed. A pellet was obtained from the supernatant by ultracentrifugation at 4 °C for 48 h. 8 mg of the pellet was mixed with 100 μL of 40 mM Finland trityl radical and a fully deuterated cryoprotecting matrix (60% glycerol-d_8, 40% D_20 volume ratio), and 36 μL was packed into a 3.2 mm zirconia rotor. Another 8 mg of the pellet was mixed with 100 μL of 40 mM Finland trityl radical in deuterated buffer, and 36 μL was packed into a 3.2 mm zirconia rotor. More details on bacteria lysate preparation can be found in the Supporting Information Section S1.

NMR Experiments. All experiments were performed using a custom-built NMR magic angle spinning (MAS) transmission line probe[35] with a Redstone (Tecmag Inc. Houston, TX) spectrometer. The Larmor frequencies of ^1H and ^{13}C at B_0 = 7.05 T were 300.179 and 75.4937 MHz, respectively. The pulse sequence was a ^{13}C rotor-synchronized Hahn echo with eDEC applied over the Hahn echo pulse sequence and the acquisition as published previously.[25] Polarization time was 7 s, and the spinning frequency was 4 kHz. The $\nu_{^{13}C}$ was 83 kHz, and TPPM ^1H decoupling had a $\nu_{^1H}$ of 83 kHz. Experiments were performed at 95 K using liquid nitrogen and at 6−7 K using liquid helium. DMFit[36] was used to fit the ^{13}C carbonyl resonance at approximately 180 ppm in each spectrum, and the resulting area under the curve was used to calculate the percent increase in area with eDEC. ^1H polarization build up times (^1H T_{1DNP}) were recorded using a saturation recovery CPMAS sequence with the $\nu_{^1H}$ used above.

Microwaves and chirped pulses were generated from a custom-built frequency-agile gyrotron.[37] For the DNP condition, the microwave frequency was 197.719 GHz. The chirped pulses were centered on the trityl EPR resonance of 197.640 GHz with a sweep width of 103 MHz and a sweep time of 13.75 μs. The incident power on the sample was 7 W, resulting in an estimated Rabi frequency (γB_{1S}) of 0.70 MHz.

A stream of liquid helium was directed at the sample centered within spinning zirconia rotors to achieve sample temperatures near 6 K, as described previously.[38] Bearing and drive were ultrahigh purity helium gas maintained at 80 K. A calibrated Cernox temperature sensor (Lake Shore Cryotronics, Inc., Westerville, OH) was used to monitor the sample temperature at the interface of the variable temperature outlet and NMR stator.[38] The temperature of the sample, incoming transfer lines, and exhaust line were monitored with a Lake Shore temperature controller.

RESULTS AND DISCUSSION

We previously demonstrated eDEC at 90 K in a model system of [U-^{13}C,^{15}N] urea using direct polarization transfer from electron spins to carbon nuclei.[25] We also performed eDEC in MAS experiments below 6 K in model systems of [U-^{13}C,^{15}N] urea and [U-^{13}C,^{15}N] L-proline using cross-polarization.[27,39] Here, we demonstrate direct carbon polarization with eDEC at 90 and 6 K in more complex biological systems including intact and lysed human Jurkat T cells and also in the soluble fraction of *E. coli* bacterial cell lysates.

eDEC on Bacterial Cell Lysates. We first performed solid effect ^{13}C-direct polarization MAS and eDEC on the purified

https://dx.doi.org/10.1021/acs.jpcb.9b10494
J. Phys. Chem. B 2020, 124, 2323−2330

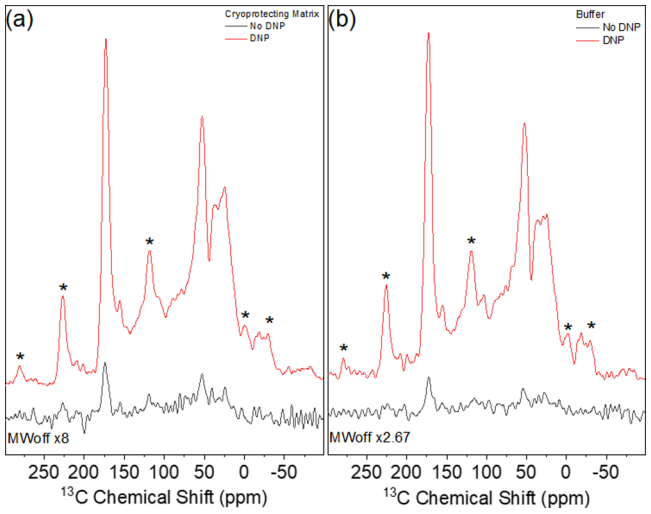

Figure 1. ^{13}C enhancements at 90 K of bacterial cell lysates with the Finland trityl radical in (a) cryoprotecting matrix (32 DNP scans, 256 no DNP scans; $\varepsilon = 35 \pm 1$) and in (b) buffer (96 DNP scans, 256 no DNP scans; $\varepsilon = 31 \pm 1$). Red represents the ^{13}C signal with DNP; black is without DNP.

soluble fraction of *E. coli* cell lysates (Figures 1 and 2) using the Finland trityl radical to analyze the effect of solvent (cryoprotecting matrix or buffer) on DNP and eDEC efficiency. At 90 K, the soluble fraction of the *E. coli* cell lysate dissolved in the cryoprotecting matrix showed a 35-fold ^{13}C enhancement of the carbonyl resonance intensity (Figure 1a). The same sample suspended in buffer provided a slightly smaller, yet significant, 31-fold enhancement (Figure 1b). This smaller enhancement was unsurprising as the glassy matrix formed with the cryoprotecting solvent is well-suited to distributing the radical and efficient DNP and thus is expected to provide a greater enhancement than a buffer solution.[30]

Similar to the lower DNP efficiency, eDEC performance in the bacteria lysate sample with a cryoprotecting matrix was also slightly less effective. At 90 K, eDEC enhanced the carbonyl resonance intensity of the lysate in a cryoprotecting matrix by $10 \pm 2\%$ (Figure 2a). The intensity of the lysate in the deuterated buffer increased by a smaller percentage of $6.0 \pm 0.1\%$ (Figure 2b).

We also investigated high sensitivity experiments by lowering the sample temperature to 6 K (Figure 2c,d). The carbonyl resonance intensity increased by 17 ± 3 and $39 \pm 0.1\%$ with eDEC for the lysates in a cryoprotecting matrix and buffer, respectively.

Interestingly, at 90 K eDEC elicits a greater increase in intensity in the lysate sample with a cryoprotecting matrix than it does with the buffer. However, at 6 K the reverse is true with a greater intensity increase occurring with the lysates with buffer. We postulate that this is due to differing polarization buildup times at each temperature. Polarization buildup times are expected to be longer at lower temperatures. Because we used the same polarization time for experiments at both temperatures, we are further from the optimal polarization time of $1.26 \times T_{1DNP}$ at 6 K than at 90 K. Thus, at 90 K we are reporting on observed spins with stronger hyperfine couplings, yielding a larger increase in intensity with eDEC in the cryoprotecting matrix, whereas the opposite is true at 6 K.

eDEC on Intact Human Cells and Human Cell Lysates. ^{13}C enhancements were recorded at 90 K to determine DNP performance to target nuclear spins within intact cells and

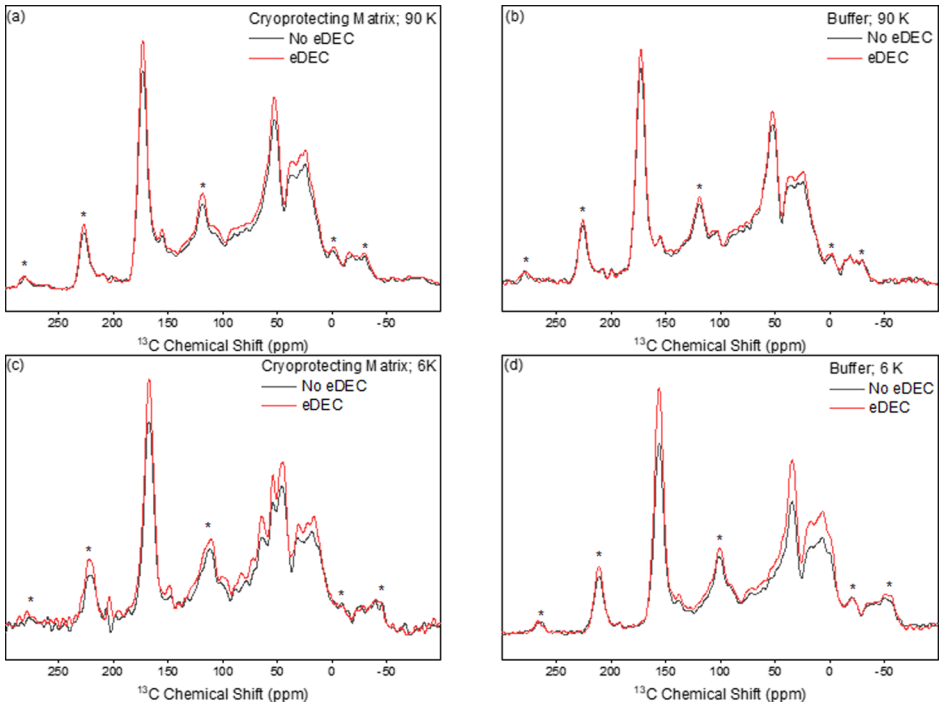

Figure 2. eDEC of bacterial cell lysates at 90 K in (a) cryoprotecting matrix (32 scans) and (b) buffer (96 scans) and at 6 K in (c) cryoprotecting matrix (4 scans) and (d) buffer (4 scans). Black represents no eDEC, while red is with eDEC. At 90 K, eDEC increased the spectrum intensity by $10 \pm 2\%$ with a cryoprotecting matrix and $6.0 \pm 0.1\%$ with the buffer. These increases were about doubled at 6 K, where the intensity increased $17 \pm 3\%$ with a cryoprotecting matrix and $39 \pm 0.1\%$ with the buffer.

https://dx.doi.org/10.1021/acs.jpcb.9b10494
J. Phys. Chem. B 2020, 124, 2323−2330

cellular lysates (Figure 4) and to probe the cellular uptake of the trityl derivatives (Figure 3). In Jurkat lysates with the

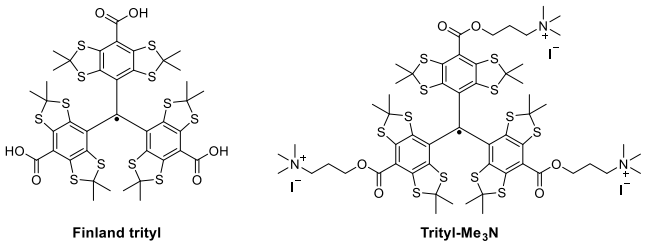

Figure 3. Chemical structures of the trityl derivatives, Finland trityl radical (left) and trityl-Me_3N (right).

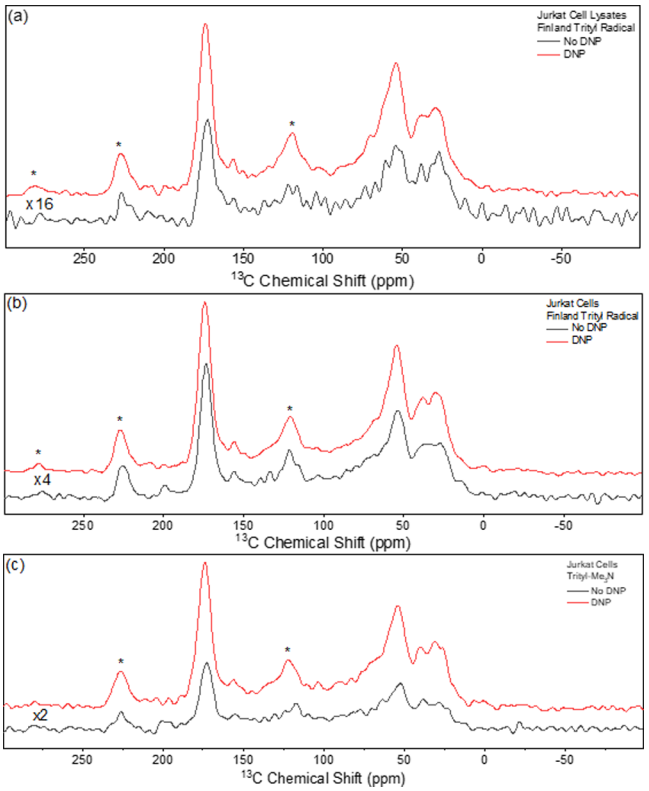

Figure 4. ^{13}C enhancements at 90 K in (a) Jurkat cell lysates with the Finland trityl radical (256 DNP scans, 4096 no DNP scans; $\varepsilon = 29.4 \pm 0.9$), (b) intact Jurkat cells with the Finland trityl radical (2560 DNP scans, 10,240 no DNP scans; $\varepsilon = 4.1 \pm 0.2$), and (c) intact Jurkat cells with trityl-Me_3N (3584 DNP scans, 6144 no DNP scans; $\varepsilon = 4.0 \pm 0.2$). Red represents the ^{13}C signal with DNP, while black is without DNP.

Finland trityl radical, nuclear spins were enhanced by a factor of 29.4 ± 0.9 (Figure 4a). In intact cells, the nuclear spins were enhanced by factors of 4.1 ± 0.2 and 4.0 ± 0.2 with the Finland trityl radical and trityl-Me_3N, respectively (Figure 4b,c). The enhancements in intact cells may be lower because of cellular localization; in the lysate, radicals are evenly distributed throughout the lysed cellular material, whereas in a cell they are likely to be subcellularly localized, limiting the number of nuclear spins in close proximity for enhancement. Further experimentation will be needed to determine the extent, if any, of the subcellular localization of the radicals. Note that the ^{13}C spectra for the Jurkat lysates and intact Jurkat cells with both radicals had the same resonances and similar relative intensities. This, along with the exceptionally short ^{1}H T_{1DNP} buildup times with both radicals (Figure 9),

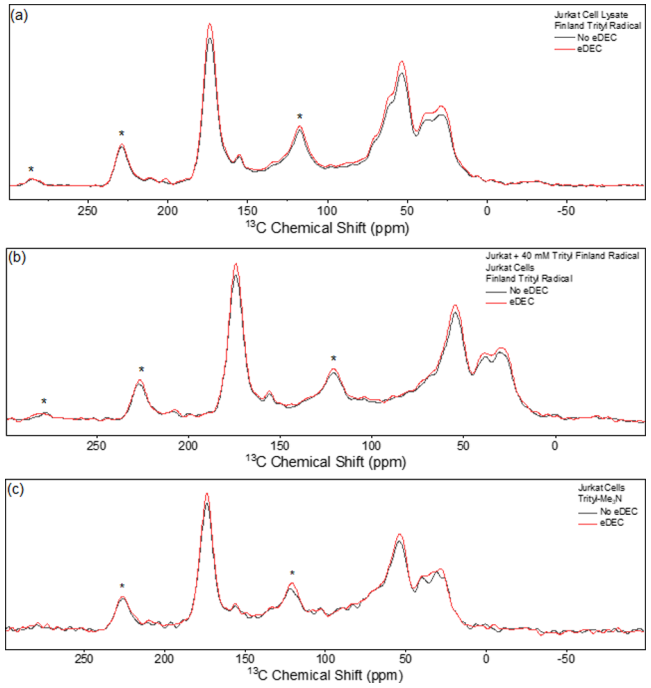

Figure 5. Comparison of DNP spectra with (red) and without (black) eDEC at 90 K for (a) Jurkat cell lysates with the Finland trityl radical (3072 scans), (b) intact Jurkat cells with the Finland trityl radical (2560 scans), and (c) intact Jurkat cells with trityl-Me_3N (3584 scans). The carbonyl resonances increased in intensity by 8.2 ± 3.2, 8.2 ± 2.8, and 8.4 ± 2.7%, respectively, with eDEC for each sample.

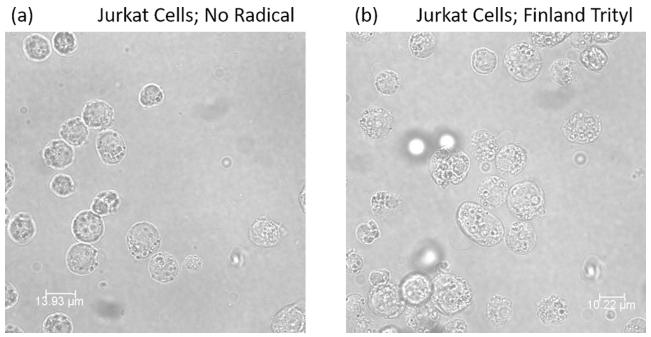

Figure 6. Light microscopy images of Jurkat cells with no radical (a), and Jurkat cells with the Finland trityl radical (b).

indicates that both radicals successfully penetrated the cellular membrane and are distributed within the cell. Further, light microscopy was performed on Jurkat cell samples with no radical and with the Trityl Finland radical to confirm that the cells were not lysed in the process of sample preparation (Figure 6).

When eDEC was applied at 90 K, the intensity of the carbonyl resonances in the Jurkat cell lysates increased by 8.2 ± 3.2% (Figure 5a), and by 8.2 ± 2.8 and 8.4 ± 2.7% in intact Jurkat cells with the Finland trityl radical and trityl-Me_3N, respectively (Figure 5b,c). This intensity improvement demonstrates that eDEC reveals nuclear spins not contributing to the NMR signal without eDEC because of paramagnetic effects. Moreover, the added cellular components do not

https://dx.doi.org/10.1021/acs.jpcb.9b10494
J. Phys. Chem. B 2020, 124, 2323−2330

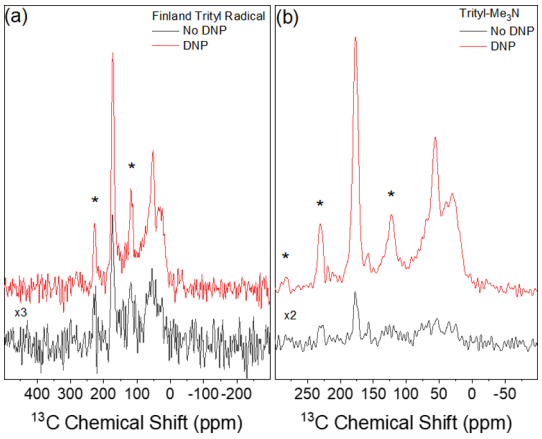

Figure 7. ^{13}C enhancements at 6 K in intact Jurkat cells with the (a) Finland trityl radical (24 DNP scans, 80 no DNP scans; $\varepsilon = 7.6 \pm 0.3$) and (b) trityl-$Me_3N$ (40 DNP scans, 80 no DNP scans; $\varepsilon = 12.5 \pm 3.8$). Red represents the ^{13}C signal with DNP, while black is without DNP.

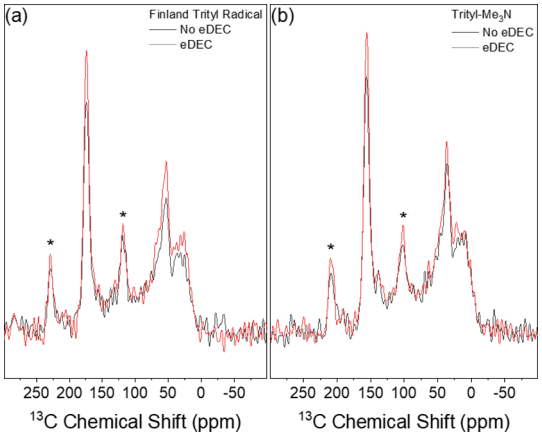

Figure 8. Comparison of DNP spectra with (red) and without (black) eDEC at 6 K for intact Jurkat cells with the (a) Finland trityl radical (24 scans) and (b) trityl-Me_3N (24 scans). The carbonyl resonances increased in intensity by 12.4 ± 3.0% and 14.5 ± 4.0%, respectively, with eDEC for each sample.

prevent eDEC, which has a similar efficiency in these more complex biological systems as in previously studied model systems.[25,27]

To further improve sensitivity and to determine the effectiveness of eDEC in intact human cells at lower temperatures, the sample temperature was reduced to below 6 K (Figures 7 and 8). Again utilizing the solid-effect DNP mechanism, there was about an 8-fold (7.6 ± 0.3) enhancement in intact Jurkat cells with the Finland trityl radical (Figure 7a) and a slightly larger 12-fold (12.5 ± 3.8) enhancement in cells with the trityl-Me_3N radical (Figure 7b). Compared to experiments at 90 K, the enhancement with the Finland trityl radical increased by a factor of 1.9 while the enhancement with trityl-Me_3N increased by a factor of 3.1. These enhancements are likely due to improved polarization transfer efficiency associated with longer spin relaxation at lower temperatures. We believe that the demonstration of eDEC in cellular samples is important, as there is no cryoprotecting matrix in the cell, and shows that it still works in this environment.

Figure 8 shows that eDEC efficiency also improved in human cells at sample temperatures below 6 K. The carbonyl resonance intensity of intact cells using the Finland trityl radical and trityl-Me_3N increased by 12.4 ± 3.0% (Figure 8a) and 14.5 ± 4.0% (Figure 8b), respectively. In addition, slight linewidth narrowing was observed in the carbonyl resonance for both trityl derivatives (see Supporting Information Figure S1).

^1H T_{1DNP} below 6 K in Human Cells. eDEC with trityl-Me_3N yielded similar results to the Finland trityl radical at 90 K, yet below 6 K, trityl-Me_3N shows a smaller increase in intensity (Figure 8), indicating that the Finland trityl radical is better suited to temperatures below 6 K. However, trityl-Me_3N has a unique advantage below 6 K (and also at 90 K) by virtue of its exceptionally short ^1H T_{1DNP} times (Figure 9). At 90 K, intact Jurkat cells with the Finland trityl radical exhibited a ^1H T_{1DNP} of 1.6 ± 0.1 s (Figure 9a), while cells with trityl-Me_3N exhibited a ^1H T_{1DNP} that was 8 times shorter at 0.2 ± 0.01 s (Figure 9b). The difference in ^1H T_{1DNP} times was similar at temperatures near 6 K: 2.7 ± 0.4 s with the Finland trityl radical and only 0.3 ± 0.01 s with trityl-Me_3N (Figure 9c,d). We note that this proton polarization buildup time of 300 ms is remarkably short and unprecedented in the literature. Although the mechanism is unclear, the methyl groups on trityl-Me_3N appear to significantly reduce the ^1H T_{1DNP}, as shown previously for bcTol and bcTol-M.[34] It is unlikely to be due to the "aggregation" common in trityl samples, as the high positive charge of the trityl-Me_3N species works to prevent this. We previously showed that in model systems, the ^1H T_{1DNP} is 19 s with the Finland trityl radical;[27] therefore, the complex cellular environment is conducive to short recovery times. Inhomogeneous distribution of the radical in the sample, which would lead to higher local concentrations of radical in these localized areas, could contribute to the shortening of the ^1H T_{1DNP} times for this radical. The short recovery times associated with the trityl-Me_3N polarizing agent are promising for extremely high sensitivity experiments below 6 K, as experiments can be repeated very quickly to yield incredible signal-to-noise per unit square root of time.[40]

CONCLUSIONS

Here, we demonstrated that the Finland trityl radical and trityl-Me_3N not only yield substantial sensitivity increases in human and bacterial cell lysates through DNP, but they can also be electron decoupled to further improve sensitivity. Furthermore, in bacterial cell lysates, these sensitivity improvements were shown to be largely independent of the sample matrix.

The intact human cells took up both trityl-based DNP polarizing agents. In these cells, DNP and eDEC successfully enhanced the sensitivity of the observed nuclear spins. Moreover, we demonstrated that NMR sensitivity in human cells can be readily improved by decreasing the sample temperature to below 6 K. The combination of DNP and eDEC at temperatures below 6 K enabled the most sensitive NMR experiments recorded to date at 7 T in intact human cells. In addition, we showed that trityl-Me_3N has extremely short ^1H T_{1DNP} times in cells, likely because of the methyl groups not present in the Finland trityl radical. At temperatures below 6 K, the ^1H T_{1DNP} time was 0.3 s, which allows for exceptionally fast repetition of experiments. This pace of data acquisition, coupled with the already superb sensitivity at 6 K with DNP and eDEC, will facilitate structural biology in the human cellular context. Moreover, eDEC implemented with

https://dx.doi.org/10.1021/acs.jpcb.9b10494
J. Phys. Chem. B 2020, 124, 2323−2330

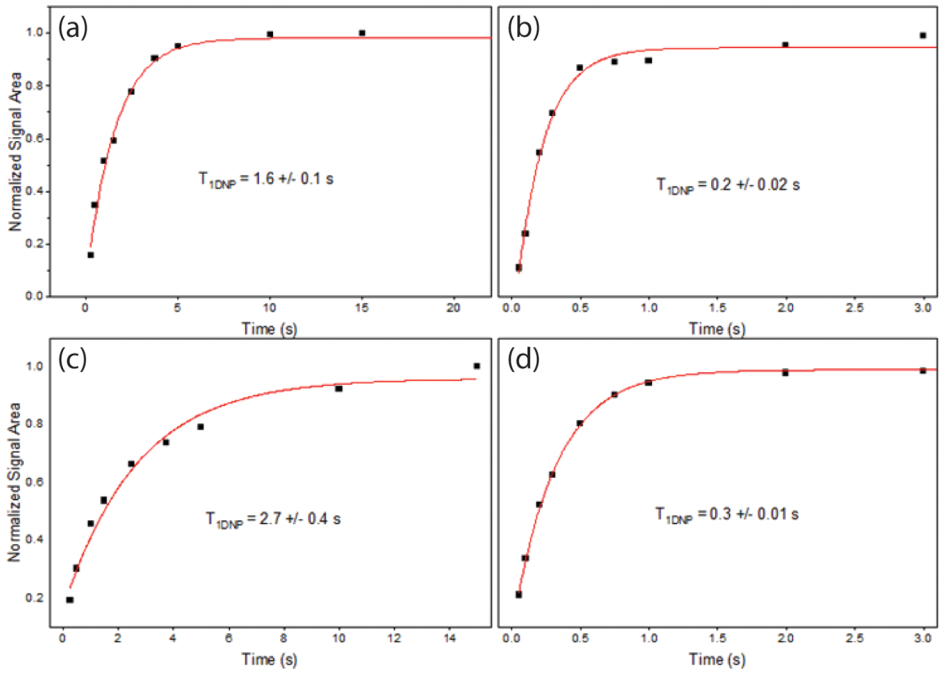

Figure 9. ^{1}H T_{1DNP} of intact Jurkat cells at 90 K with the Finland trityl radical (a) and trityl-Me_3N (b) and at 6 K with the Finland trityl radical (c) and trityl-Me_3N (d).

multidimensional NMR will provide the sensitivity enhancements and spectral resolution required for the analysis of complex biological systems. Finally, we note that future implementation of DNP and eDEC for in-cell NMR will realize the ability to target radicals to specific sites of structural interest.

■ ASSOCIATED CONTENT

Supporting Information

The Supporting Information is available free of charge at https://pubs.acs.org/doi/10.1021/acs.jpcb.9b10494.

The synthesis and characterization of trityl-Me_3N, bacterial cell lysate preparation, and eDEC on intact human cells at 6 K (PDF)

■ AUTHOR INFORMATION

Corresponding Author

Alexander B. Barnes − *Department of Chemistry, Washington University in St. Louis, St. Louis, Missouri 63130, United States;* orcid.org/0000-0003-3748-8508; Email: barnesab@wustl.edu

Authors

Patrick T. Judge − *Department of Chemistry and Department of Biochemistry, Biophysics & Structural Biology, Washington University in St. Louis, St. Louis, Missouri 63130, United States*

Erika L. Sesti − *Department of Chemistry, Washington University in St. Louis, St. Louis, Missouri 63130, United States*

Lauren E. Price − *Department of Chemistry, Washington University in St. Louis, St. Louis, Missouri 63130, United States*

Brice J. Albert − *Department of Chemistry, Washington University in St. Louis, St. Louis, Missouri 63130, United States*

Nicholas Alaniva − *Department of Chemistry, Washington University in St. Louis, St. Louis, Missouri 63130, United States*

Edward P. Saliba − *Department of Chemistry, Washington University in St. Louis, St. Louis, Missouri 63130, United States*

Thomas Halbritter − *Department of Chemistry, Science Institute, University of Iceland, 107 Reykjavik, Iceland*

Snorri Th. Sigurdsson − *Department of Chemistry, Science Institute, University of Iceland, 107 Reykjavik, Iceland;* orcid.org/0000-0003-2492-1456

George B. Kyei − *Department of Medicine, Washington University School of Medicine, St. Louis, Missouri 63130, United States; Noguchi Memorial Institute for Medical Research, College of Health Sciences, University of Ghana, Accra 02233, Ghana*

Complete contact information is available at: https://pubs.acs.org/10.1021/acs.jpcb.9b10494

Author Contributions

These authors contributed equally. The manuscript was written through contributions of all authors. All authors have given approval to the final version of the manuscript.

Notes

The authors declare the following competing financial interest(s): A.B.B. is the author of a patent related to this work filed by the Washington University in Saint Louis (WO2015175507A1).

A.B.B. is the author of a patent related to this work filed by the Washington University in Saint Louis (WO 2015175507 A1).

■ ACKNOWLEDGMENTS

This work received financial support from the National Institutes of Health (NIH) in the form of the grant DP2-GM119131, the National Science Foundation in the form of the grant NSF-IDBR (CAREER DBI-1553577), and the Camille Dreyfus Teacher-Scholar Awards Program. We thank Chukun Gao, Faith Scott, and Pin-Hui Chen for helpful discussions.

REFERENCES

(1) Polenova, T.; Gupta, R.; Goldbourt, A. Magic Angle Spinning NMR Spectroscopy: A Versatile Technique for Structural and Dynamic Analysis of Solid-Phase Systems. *Anal. Chem.* **2015**, *87*, 5458−5469.

(2) Kaplan, M.; Narasimhan, S.; de Heus, C.; Mance, D.; van Doorn, S.; Houben, K.; Popov-Čeleketić, D.; Damman, R.; Katrukha, E. A.; Jain, P.; et al. EGFR Dynamics Change during Activation in Native Membranes as Revealed by NMR. *Cell* **2016**, *167*, 1241−1251.

(3) Mak-Jurkauskas, M. L.; Bajaj, V. S.; Hornstein, M. K.; Belenky, M.; Griffin, R. G.; Herzfeld, J. Energy Transformations Early in the Bacteriorhodopsin Photocycle Revealed by DNP-Enhanced Solid-State NMR. *Proc. Natl. Acad. Sci. U.S.A.* **2008**, *105*, 883−888.

(4) Selenko, P.; Wagner, G. Looking into Live Cells with In-Cell NMR Spectroscopy. *J. Struct. Biol.* **2007**, *158*, 244−253.

(5) Wylie, B. J.; Dzikovski, B. G.; Pawsey, S.; Caporini, M.; Rosay, M.; Freed, J. H.; McDermott, A. E. Dynamic Nuclear Polarization of Membrane Proteins: Covalently Bound Spin-Labels at Protein-Protein Interfaces. *J. Biomol. NMR* **2015**, *61*, 361−367.

(6) Ceccon, A.; Tugarinov, V.; Bax, A.; Clore, G. M. Global Dynamics and Exchange Kinetics of a Protein on the Surface of Nanoparticles Revealed by Relaxation-Based Solution NMR Spectroscopy. *J. Am. Chem. Soc.* **2016**, *138*, 5789−5792.

(7) Gupta, R.; Lu, M.; Hou, G.; Caporini, M. A.; Rosay, M.; Maas, W.; Struppe, J.; Suiter, C.; Ahn, J.; Byeon, I.-J. L.; et al. Dynamic Nuclear Polarization Enhanced MAS NMR Spectroscopy for Structural Analysis of HIV-1 Protein Assemblies. *J. Phys. Chem. B* **2016**, *120*, 329−339.

(8) Lilly Thankamony, A. S.; Wittmann, J. J.; Kaushik, M.; Corzilius, B. Dynamic Nuclear Polarization for Sensitivity Enhancement in Modern Solid-State NMR. *Prog. Nucl. Magn. Reson. Spectrosc.* **2017**, *102*−*103*, 120−195.

(9) Saliba, E. P.; Sesti, E. L.; Alaniva, N.; Barnes, A. B. Pulsed Electron Decoupling and Strategies for Time Domain Dynamic Nuclear Polarization with Magic Angle Spinning. *J. Phys. Chem. Lett.* **2018**, *9*, 5539−5547.

(10) Dale, M. W.; Wedge, C. J. Optically Generated Hyperpolarization for Sensitivity Enhancement in Solution-State NMR Spectroscopy. *Chem. Commun.* **2016**, *52*, 13221−13224.

(11) Maly, T.; Debelouchina, G. T.; Bajaj, V. S.; Hu, K.-N.; Joo, C.-G.; Mak-Jurkauskas, M. L.; Sirigiri, J. R.; van der Wel, P. C. A.; Herzfeld, J.; Temkin, R. J.; et al. Dynamic Nuclear Polarization at High Magnetic Fields. *J. Chem. Phys.* **2008**, *128*, 052211.

(12) Thurber, K. R.; Yau, W.-M.; Tycko, R. Low-Temperature Dynamic Nuclear Polarization at 9.4 T with a 30 MW Microwave Source. *J. Magn. Reson.* **2010**, *204*, 303−313.

(13) Becerra, L. R.; Gerfen, G. J.; Temkin, R. J.; Singel, D. J.; Griffin, R. G. Dynamic Nuclear Polarization with a Cyclotron Resonance Maser at 5 T. *Phys. Rev. Lett.* **1993**, *71*, 3561−3564.

(14) Hall, D. A.; Maus, D. C.; Gerfen, G. J.; Inati, S. J.; Becerra, L. R.; Dahlquist, F. W.; Griffin, R. G. Polarization-Enhanced NMR Spectroscopy of Biomolecules in Frozen Solution. *Science* **1997**, *276*, 930−932.

(15) Overhauser, A. W. Polarization of Nuclei in Metals. *Phys. Rev.* **1953**, *92*, 411.

(16) Barnes, A. B.; Nanni, E. A.; Herzfeld, J.; Griffin, R. G.; Temkin, R. J. 250 GHz Gyrotron with a 3 GHz Tuning Bandwidth for Dynamic Nuclear Polarization Alexander. *J. Magn. Reson.* **2012**, *221*, 147−153.

(17) Smith, A. N.; Caporini, M. A.; Fanucci, G. E.; Long, J. R. A Method for Dynamic Nuclear Polarization Enhancement of Membrane Proteins. *Angew. Chem., Int. Ed.* **2015**, *54*, 1542−1546.

(18) Franck, J. M.; Pavlova, A.; Scott, J. A.; Han, S. Quantitative Cw Overhauser Effect Dynamic Nuclear Polarization for the Analysis of Local Water Dynamics. *Prog. Nucl. Magn. Reson. Spectrosc.* **2013**, *74*, 33−56.

(19) Bajaj, V. S.; Mak-Jurkauskas, M. L.; Belenky, M.; Herzfeld, J.; Griffin, R. G. Functional and Shunt States of Bacteriorhodopsin Resolved by 250 GHz Dynamic Nuclear Polarization-Enhanced Solid-State NMR. *Proc. Natl. Acad. Sci. U.S.A.* **2009**, *106*, 9244−9249.

(20) Equbal, A.; Li, Y.; Leavesley, A.; Huang, S.; Rajca, S.; Rajca, A.; Han, S. Truncated Cross Effect Dynamic Nuclear Polarization: An Overhauser Effect Doppelgänger. *J. Phys. Chem. Lett.* **2018**, *9*, 2175−2180.

(21) Lange, S.; Linden, A. H.; Akbey, Ü.; Trent Franks, W.; Loening, N. M.; Rossum, B.-J. v.; Oschkinat, H. The Effect of Biradical Concentration on the Performance of DNP-MAS-NMR. *J. Magn. Reson.* **2012**, *216*, 209−212.

(22) Mentink-Vigier, F.; Paul, S.; Lee, D.; Feintuch, A.; Hediger, S.; Vega, S.; De Paëpe, G. Nuclear Depolarization and Absolute Sensitivity in Magic-Angle Spinning Cross Effect Dynamic Nuclear Polarization. *Phys. Chem. Chem. Phys.* **2015**, *17*, 21824−21836.

(23) Thurber, K. R.; Tycko, R. Perturbation of Nuclear Spin Polarizations in Solid State NMR of Nitroxide-Doped Samples by Magic-Angle Spinning without Microwaves. *J. Chem. Phys.* **2014**, *140*, 184201.

(24) Corzilius, B.; Andreas, L. B.; Smith, A. A.; Ni, Q. Z.; Griffin, R. G. Paramagnet Induced Signal Quenching in MAS − DNP Experiments in Frozen Homogeneous Solutions. *J. Magn. Reson.* **2014**, *240*, 113−123.

(25) Saliba, E. P.; Sesti, E. L.; Scott, F. J.; Albert, B. J.; Choi, E. J.; Alaniva, N.; Gao, C.; Barnes, A. B. Electron Decoupling with Dynamic Nuclear Polarization in Rotating Solids. *J. Am. Chem. Soc.* **2017**, *139*, 6310−6313.

(26) Lee, D.; Bouleau, E.; Saint-Bonnet, P.; Hediger, S.; De Paëpe, G. Ultra-Low Temperature MAS-DNP. *J. Magn. Reson.* **2016**, *264*, 116−124.

(27) Sesti, E. L.; Saliba, E. P.; Alaniva, N.; Barnes, A. B. Electron Decoupling with Cross Polarization and Dynamic Nuclear Polrization Below 6 K. *J. Magn. Reson.* **2018**, *295*, 1−5.

(28) Frederick, K. K.; Michaelis, V. K.; Corzilius, B.; Ong, T.-C.; Jacavone, A. C.; Griffin, R. G.; Lindquist, S. Sensitivity-Enhanced NMR Reveals Alterations in Protein Structure by Cellular Milieus. *Cell* **2015**, *163*, 620−628.

(29) Latham, M. P.; Kay, L. E. Is Buffer a Good Proxy for a Crowded Cell-Like Environment? A Comparative NMR Study of Calmodulin Side-Chain Dynamics in Buffer and E. Coli Lysate. *PLoS One* **2012**, *7*, No. e48226.

(30) Leavesley, A.; Wilson, C. B.; Sherwin, M.; Han, S. Effect of Water/Glycerol Polymorphism on Dynamic Nuclear Polarization. *Phys. Chem. Chem. Phys.* **2018**, *20*, 9897−9903.

(31) Albert, B. J.; Gao, C.; Sesti, E. L.; Saliba, E. P.; Scott, F. J.; Sigurdsson, S. T.; Barnes, A. B. Dynamic Nuclear Polarization NMR in Human Cells Using Fluorescent Polarizing Agents. *Biochemistry* **2018**, *57*, 4741−4746.

(32) Trukhin, D. V.; Rogozhnikova, O. Y.; Troitskaya, T. I.; Kuzhelev, A. A.; Amosov, E. V.; Halpern, H. J.; Koval', V. V.; Tormyshev, V. M. New Spin Probes: Tri- and Hexacationic Derivatives of Stable Tetrathiatriarylmethyl Radicals. *Russ. J. Org. Chem.* **2019**, *55*, 296−301.

(33) Dhimitruka, I.; Grigorieva, O.; Zweier, J. L.; Khramtsov, V. V. Synthesis, Structure, and EPR Characterization of Deuterated Derivatives of Finland Trityl Radical. *Bioorg. Med. Chem. Lett.* **2010**, *20*, 3946−3949.

(34) Geiger, M.-A.; Jagtap, A. P.; Kaushik, M.; Sun, H.; Stöppler, D.; Sigurdsson, S. T.; Corzilius, B.; Oschkinat, H. Efficiency of Water-Soluble Nitroxide Biradicals for Dynamic Nuclear Polarization in Rotating Solids at 9 . 4 T : BcTol-M and Cyolyl-TOTAPOL as New Polarizing Agents. *Chem.—Eur. J.* **2018**, *24*, 13485−13494.

(35) Scott, F. J.; Alaniva, N.; Golota, N. C.; Sesti, E. L.; Saliba, E. P.; Price, L. E.; Albert, B. J.; Chen, P.; O'Connor, R. D.; Barnes, A. B. A Versatile Custom Cryostat for Dynamic Nuclear Polarization Supports Multiple Cryogenic Magic Angle Spinning Transmission Line Probes. *J. Magn. Reson.* **2018**, *297*, 23−32.

(36) Massiot, D.; Fayon, F.; Capron, M.; King, I.; Le Calvé, S.; Alonso, B.; Durand, J.-O.; Bujoli, B.; Gan, Z.; Hoatson, G. Modelling

https://dx.doi.org/10.1021/acs.jpcb.9b10494
J. Phys. Chem. B 2020, 124, 2323−2330

One- and Two-Dimensional Solid-State NMR Spectra. *Magn. Reson. Chem.* **2002**, *40*, 70−76.
(37) Scott, F. J.; Saliba, E. P.; Albert, B. J.; Alaniva, N.; Sesti, E. L.; Gao, C.; Golota, N. C.; Choi, E. J.; Jagtap, A. P.; Wittmann, J. J.; et al. Frequency-Agile Gyrotron for Electron Decoupling and Pulsed Dynamic Nuclear Polarization. *J. Magn. Reson.* **2018**, *289*, 45−54.
(38) Sesti, E. L.; Alaniva, N.; Rand, P. W.; Choi, E. J.; Albert, B. J.; Saliba, E. P.; Scott, F. J.; Barnes, A. B. Magic Angle Spinning NMR below 6 K with a Computational Fluid Dynamics Analysis of Fluid Flow and Temperature Gradients. *J. Magn. Reson.* **2018**, *286*, 1−9.
(39) Alaniva, N.; Saliba, E. P.; Sesti, E. L.; Judge, P. T.; Barnes, A. B. Electron Decoupling with Chirped Microwave Pulses for Rapid Signal Acquisition and Electron Saturation Recovery. *Angew. Chem., Int. Ed.* **2019**, *58*, 7259.
(40) Bouleau, E.; Saint-bonnet, P.; Mentink-vigier, F.; Takahashi, H.; Jacquot, J.-F.; Bardet, M.; Aussenac, F.; Purea, A.; Engelke, F.; Hediger, S.; et al. Chemical Science Pushing NMR Sensitivity Limits Using Dynamic Nuclear Polarization with Closed-Loop Cryogenic Helium Sample Spinning. *Chem. Sci.* **2015**, *6*, 6806−6812.

https://dx.doi.org/10.1021/acs.jpcb.9b10494
J. Phys. Chem. B 2020, 124, 2323−2330